View metadata, citation and similar papers at core.ac.uk

brought to you by CORE

provided by Xiamen University Institutional Repository

Analyst

COMMUNICATION

View Article Online
View Journal | View Issue

# A fluorescent switch for sequentially and selectively sensing copper(II) and L-histidine *in vitro* and in living cells†

Cite this: *Analyst*, 2014, **139**, 3360

Received 27th February 2014
Accepted 16th April 2014

DOI: 10.1039/c4an00410h

www.rsc.org/analyst

Xiaojing Wang,[a] Qingqing Miao,[a] Tingjie Song,[c] Qingpan Yuan,[a] Jinhao Gao[b] and Gaolin Liang*[ab]

Published on 17 April 2014. Downloaded by University of Science and Technology of China on 12/01/2015 02:05:50.

Herein, we report the development of a new fluorescent switch for sequential and selective sensing of $Cu^{2+}$ and L-histidine (L-His) *in vitro* and in living cells for the first time. In the absence of metal ions, Ac-SAACQ-Gly-Gly-Gly-Lys (FITC) (**1**) exhibits comparable fluorescence to that of free FITC. In the presence of metal ions, **1** selectively coordinates to $Cu^{2+}$, causing its fluorescence emission to be quenched *via* photoinduced electron transfer. Interestingly, the as-formed **1**–$Cu^{2+}$ complex selectively responds to L-His among the 20 natural amino acids by turning its fluorescence on. This property of fluorescence switch of **1** was successfully applied for qualitatively and quantitatively sensing $Cu^{2+}$ and L-His *in vitro*. Using this dual functional probe, we also sequentially imaged $Cu^{2+}$ and L-His in living HepG2 cells. Our new probe **1** could be applied for not only environmental monitoring but also biomolecule detection in the near future.

Copper ions ($Cu^{2+}$) play a key role in many physiological processes including gene expression and protein functioning,[1] and are also required by the human nervous system.[2] Copper deficiency is associated with myelopathy[3] but high levels of $Cu^{2+}$ may lead to the damage of liver or kidney.[4] To date, a tremendous number of methods have been developed for the detection of copper.[5] For example, traditional instrument-assisted technologies such as inductively coupled plasma mass spectroscopy (ICPMS)[6] and atomic absorption/emission spectroscopy (AAS/AES)[7] have been applied for the detection of $Cu^{2+}$ as standard methodologies. The newly developed instrument-assisted techniques based on surface plasmon resonance (SPR)[8] or surface-enhanced Raman scattering (SERS)[9] were also successfully applied for the detection of $Cu^{2+}$ with high sensitivity. However, the requirement of sophisticated, expensive equipment, and highly trained personnel for the aforementioned techniques restricts their application in the facile and practical detection of $Cu^{2+}$. This calls for new methods and many small molecule-based (SMB) systems had been developed for this purpose. For example, new "off" (or "on") fluorescent probes[10] or nucleic acid sensors[11] have been developed for the detection of $Cu^{2+}$ with high sensitivity. Nevertheless, there are still some limitations in these systems including tedious procedures of sample preparation, rigid reaction conditions, low accuracy due to the chemical/physical interference from similarities of coexisting metal ion species,[12] aggregation of the probes at micromolar concentrations,[10i] or poor biocompatibility.[10j]

L-Histidine (L-His, HisH) in the form of free amino acid (AA) acts as a tridentate ligand toward transition-metal ions.[13] Since the discovery of $Cu^{2+}$–L-His species in human blood and their treatment for Menkes disease (a fatal genetic neurodegenerative disease), a great deal of interest has been generated.[14] Recently, using $Cu^{2+}$–L-His to treat infantile hypertrophic cardioencephalomyopathy has also been reported.[15] To date, extensive research efforts have been made to determine the role of L-His in cellular uptake of copper. Nevertheless, few sensors have been developed for successful detection of L-His due to their either poor selectivity or low limit of detection for L-His among the 20 natural AAs.[16]

Encouraged by these, as shown in Fig. 1, we designed a fluorescent switch using a water soluble probe Ac-SAACQ-Gly-Gly-Gly-Lys (FITC)-OH (**1**) for the sequential detection of $Cu^{2+}$ and L-His *in vitro* and in living cells with high selectivity for the first time. The $Cu^{2+}$-binding motif used in this work is a lysine-derived quinoline, referred to as a single AA chelate quinoline (SAACQ), first reported by Valliant and his co-workers.[17] Unlike those fluorescent probes which directly conjugate with $Cu^{2+}$

[a]*CAS Key Laboratory of Soft Matter Chemistry, Department of Chemistry & Collaborative Innovation Center of Suzhou Nano Science and Technology, University of Science and Technology of China, 96 Jinzhai Road, Hefei, Anhui 230026, China. E-mail: gliang@ustc.edu.cn; Fax: +86-551-63600730; Tel: +86-551-63607935*

[b]*State Key Laboratory of Physical Chemistry of Solid Surfaces, College of Chemistry and Chemical Engineering, Xiamen University, Xiamen 361005, China*

[c]*CAS Key Laboratory of Soft Matter Chemistry, Department of Polymer Science and Engineering, University of Science and Technology of China, 96 Jinzhai Road, Hefei, Anhui 230026, China*

† Electronic supplementary information (ESI) available: Experimental methods and details, syntheses and characterization of Fmoc-SAACQ, **1a**, **1b**, and **1**, HPLC conditions, UV-vis, fluorescence, NMR, cell imaging, supplementary schemes, tables, and figures (Schemes S1 and S2, Table S1, Fig. S1–S17). See DOI: 10.1039/c4an00410h



This journal is © The Royal Society of Chemistry 2014

Published on 17 April 2014. Downloaded by University of Science and Technology of China on 12/01/2015 02:05:50.

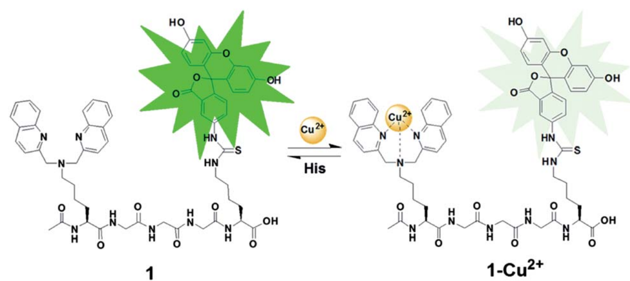


Fig. 1 Schematic illustration of a fluorescent switch for the sequential detection of $Cu^{2+}$ and L-His.

resulting in fluorescence "off" for irreversible detection of $Cu^{2+}$, we separated the $Cu^{2+}$-binding motif (*i.e.*, SAACQ) from the fluorophore (herein FITC) due to the following two reasons. First, the separated SAACQ–$Cu^{2+}$ complex still can quench the fluorescence of FITC *via* photoinduced electron transfer (PET).[18] Secondly, the separated SAACQ–$Cu^{2+}$ complex has good accessibility to L-His. Thus, the subsequent competitive binding of $Cu^{2+}$ with L-His leads to the disassociation of the SAACQ–$Cu^{2+}$ complex, resulting in the fluorescence recovery of **1** for L-His detection. Between the SAACQ–$Cu^{2+}$ complex and FITC, we put Gly-Gly-Gly-Lys (GGGK) as the shortest linker to ensure the water solubility and biocompatibility of **1** while in the meantime retain its PET effect. Moreover, since the SAACQ can be regarded as a natural AA, the Ac-SAACQ-Gly-Gly-Gly-Lys-OH backbone for **1** could be synthesized in one-step with solid phase peptide synthesis (SPPS) (Fig. S1 and S3 and Scheme S1, ESI†). Interestingly, we found that this water soluble, dual functional probe **1** is selectively sensitive to $Cu^{2+}$ and L-His, suggesting its importance for biomolecule detection.[19]

The aforementioned probe **1** contains two segments: the non-fluorescent Ac-SAACQ-Gly-Gly-Gly-Lys-OH (**1b**) backbone for $Cu^{2+}$ chelation and the fluorophore fluorescein isothiocyanate (FITC) (Fig. 1 and Scheme S2, ESI†). Compared with free FITC under the same conditions, our probe **1** exhibited 69.6% fluorescence intensity (FI) of that of free FITC (3373 *vs.* 4844, Fig. S4, ESI†), suggesting that the modification of FITC with **1b** does not induce an obvious decrease of the FI of the fluorophore. Upon addition of 20 μM $Cu^{2+}$ at room temperature (RT), both spectroscopic and photographic fluorescence of 10 μM **1** in Tris–HCl buffered (pH 7.5, 50 mM) solution dramatically decreased (Fig. 2 and Fig. S5, ESI†). To ensure that the FI decrease of **1** resulted from the coordination between $Cu^{2+}$ and SAACQ instead of the direct binding of $Cu^{2+}$ to FITC, we measured the UV-vis and fluorescence spectra of **1b**, FITC, and **1** before and after $Cu^{2+}$ addition. The results showed that addition of $Cu^{2+}$ did not induce obvious changes of either the UV-vis or the fluorescence spectra of FITC, but did induce changes of both of **1** and changes of the UV-vis spectra of **1b** (Fig. S6, ESI†). This indicated that it is the coordination of $Cu^{2+}$ to SAACQ on **1** that stabilizes the metal ion in the proximity of fluorophore FITC, thus quenching the fluorescence of FITC.

In addition to the 6 nm blue-shift of UV-vis spectra at 498 nm of **1** after $Cu^{2+}$ addition (Fig. S6, ESI†), we also conducted

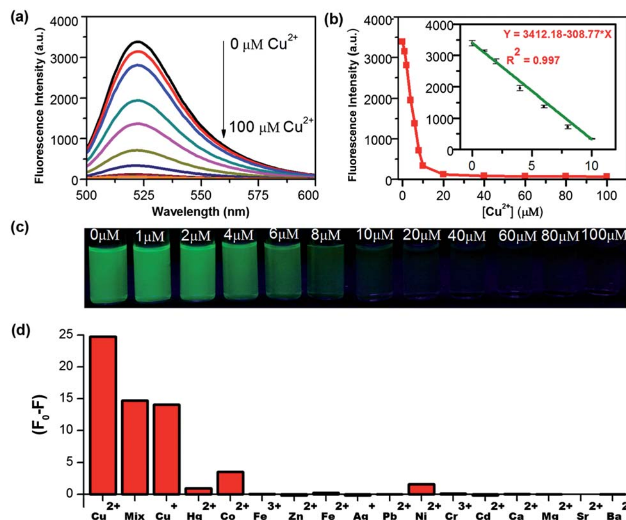


Fig. 2 (a) Fluorescence spectra of probe **1** (10 μM, $\lambda_{ex} = 465$ nm) in the presence of various concentrations of $Cu^{2+}$ (0, 1, 2, 4, 8, 10, 20, 40, 60, 80, and 100 μM) in Tris–HCl buffered (pH 7.5, 50 mM) aqueous solution at RT. (b) Correlation of $\Delta FI_{521\ nm}$ in part (a) with $Cu^{2+}$ concentration between 0 and 100 μM. The inset shows a fitted calibration line in the liner region of 0–10 μM $Cu^{2+}$. The error bar represents the standard deviation of three measurements. (c) The corresponding fluorescence images of **1** in a cuvette in the presence of different concentrations of $Cu^{2+}$ under a UV lamp. (d) Competitive selectivity of 10 μM **1** in the presence of $Cu^{2+}$ (2 equiv.), mixture, 2 equiv. of $Cu^{+}$, $Hg^{2+}$, $Co^{2+}$, $Fe^{3+}$, $Zn^{2+}$, $Fe^{2+}$, $Ag^{+}$, $Pb^{2+}$, $Ni^{2+}$, $Cr^{3+}$, $Cd^{2+}$, $Ca^{2+}$, $Mg^{2+}$, $Sr^{2+}$, $Ba^{2+}$ respectively. Emission: 521 nm.

$^1$HNMR and electrospray ionization mass (ESI-MS) spectroscopic analyses to confirm the coordination between SAACQ and $Cu^{2+}$. For $^1$HNMR spectroscopic analysis, fluorenylmethyloxycarbonyl-SAACQ (Fmoc-SAACQ) was used as a model compound. Since $Cu^{2+}$ is a paramagnetic ion which heavily interferes with $^1$HNMR signals, we then chose $Zn^{2+}$ as an alternative of $Cu^{2+}$ to study its coordination with Fmoc-SAACQ.[20] $^1$HNMR spectra of Fmoc-SAACQ showed that the proton resonances on the quinoline rings were shifted downfield and became broader upon the addition of 2 equiv. of $ZnCl_2$, indicating the coordination of $Zn^{2+}$ to Fmoc-SAACQ (Fig. S7, ESI†). This indicates that the coordination reduces the conformational degrees of freedom of the two quinoline moieties and inhibits their intramolecular π–π stacking. ESI-MS spectra of **1** upon addition of $Cu^{2+}$ clearly showed that there are two major peaks of *m*/*z* 1222.34 and 611.62, which have typical isotopic peaks similar to those of $Cu^{2+}$, corresponding to $[\mathbf{1}\text{–Cu}]^{+}$ and $[\mathbf{1}\text{–Cu}]^{2+}$ respectively (Fig. S8, ESI†). The above results echoed that the FI decrease of **1** upon $Cu^{2+}$ addition was induced by the coordination between the copper ions and quinoline moieties and therefore the FI of FITC was quenched *via* the PET mechanism. Under these conditions, a 1 : 1 probe copper stoichiometry is assumed, and the binding constant ($K_s$) of probe **1** with $Cu^{2+}$ was calculated to be $1.5 \times 10^5\ M^{-1}$ (Fig. S9, ESI†). It was reported that the binding constant of L-His towards $Cu^{2+}$ is $1 \times 10^8$ to $1.3 \times 10^{10}$ (Table S2†),[13c] much larger than that of our probe **1**. Thus, using the **1**–$Cu^{2+}$ complex for the

Published on 17 April 2014. Downloaded by University of Science and Technology of China on 12/01/2015 02:05:50.

following L-His detection becomes feasible. On the other hand, it is infeasible for **1** to detect $Cu^{2+}$ which is already pre-complexed with L-His.

Fig. 2a shows the fluorescence spectra of 10 μM **1** before and after the addition of different concentrations of $Cu^{2+}$ at RT in Tris–HCl buffered (pH 7.5, 50 mM) solution for 5 min. In general, the fluorescence of **1** decreases with the increase of $Cu^{2+}$ concentration. The fluorescence images of **1** in a cuvette under a UV lamp, corresponding to these changes, are shown in Fig. 2c. By correlating the fluorescence change at 521 nm (*i.e.*, $F_0 - F$, $\Delta F_{521\ nm}$) with the concentration of $Cu^{2+}$, we obtained a calibration curve for the determination of $Cu^{2+}$ *in vitro*. As shown in Fig. 2b, a linear relationship between the $\Delta F_{521\ nm}$ and $Cu^{2+}$ concentration ($Y = 3412.18 - 308.77X$, $R^2 = 0.997$) was obtained over the range of 0–10 μM. The limit of detection (LOD) of $Cu^{2+}$ of this assay is 0.24 μM ($S/N = 3$), which is satisfactorily below the limit of $Cu^{2+}$ in drinking water set by the U.S. Environmental Protection Agency (EPA) (~20 μM),[5c] but far exceeds the concentration of free copper ions in an unstressed cell (about $10^{-18}$ M).[21]

Selectivity is one of the important parameters to evaluate the performance of a new fluorescent probe. Particularly, for a cellular imaging probe which potentially has biomedical or environmental applications, a highly selective response to the target over other potentially competing species is a necessity. Therefore, the selectivity study of **1** to $Cu^{2+}$ over various metal ions such as abundant cellular cations (*e.g.*, $Ca^{2+}$ and $Mg^{2+}$), essential metal ions in cells (*e.g.*, $Co^{2+}$, $Fe^{3+}$, $Zn^{2+}$, $Fe^{2+}$, $Ni^{2+}$, $Sr^{2+}$, $Ba^{2+}$), and environmentally relevant heavy metal ions (*e.g.*, $Hg^{2+}$, $Ag^{+}$, $Pb^{2+}$, $Cr^{3+}$, $Cd^{2+}$), was conducted. As shown in Fig. 2d, mixing the 10 μM **1** with 20 μM $Cu^{2+}$ induced a fluorescence change ratio of **1** at 521 nm, *i.e.*, $(F_0 - F)/F$) as large as 24.8. However, separately mixing 10 μM **1** with other above-mentioned metal ions at 20 μM did not induce an obvious FL change ratio (the highest is 3.5 for $Co^{2+}$ except $Cu^{+}$). Interestingly, mixing 10 μM **1** with all the metal ions studied (including $Cu^{2+}$) at 20 μM induced a FI change ratio of 14.6, suggesting that **1** has good selectivity to $Cu^{2+}$ even under the heavy interference of other fourteen metal ions. These excellent features of **1** warrant its potential applications in environmental monitoring and biomolecule detection.

Since L-amino acids (L-AAs) play a key role in the diagnosis and treatment of disease, many efforts have been made to develop feasible approaches for their detection.[13a,22] Among the 20 natural AAs, L-His is very important and well known for its chelation properties with metal ions such as $Ni^{2+}$. Therefore, in this study, we also applied **1** for sequential detection of L-His after its coordination to $Cu^{2+}$. As shown in Fig. 3a, after the formation of the **1**–$Cu^{2+}$ complex, progressive addition of L-His to the system gradually turned the fluorescence "on". This indicated that L-His competitively binds with $Cu^{2+}$ in the **1**–$Cu^{2+}$ complex by forming a more stable complex $Cu^{2+}$–L-His, freeing **1** from the complex and thus recovering its fluorescence. By correlating the fluorescence change ratio at 521 nm (*i.e.*, $(F - F_0)/F_0$) with the concentration of L-His, we obtained a calibration curve for the determination of L-His *in vitro*. As shown in Fig. S10,† a linear relationship between the $(F - F_0)/F_0$ and L-His

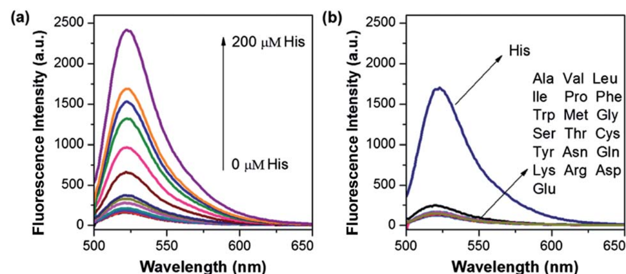


Fig. 3 (a) Fluorescence spectra of **1**–$Cu^{2+}$ complex (10 μM **1** and 10 μM $Cu^{2+}$) upon addition of various concentrations of L-His (0, 1, 2, 4, 8, 10, 20, 40, 60, 80, 100, and 200 μM) in Tris–HCl buffered aqueous solution (pH 7.5, 50 mM) at RT. The fitted calibration line in the linear region of 1–60 μM of L-His (Fig S10, ESI†). (b) Selectivity study of the **1**–$Cu^{2+}$ complex (10 μM **1** and 20 μM $Cu^{2+}$) to L-His among the twenty natural AAs (100 μM for each).

concentration ($Y = -0.22301 + 0.13376X$, $R^2 = 0.959$) was obtained over the range of 1–60 μM. The LOD of L-His of this assay is 1.6 μM ($S/N = 3$). Surprisingly, the fluorescence of the **1**–$Cu^{2+}$ complex could only be turned "on" by L-His among the 20 natural AAs, suggesting a great selectivity of this system for L-His detection (Fig. 3b).

The excellent property of fluorescence switch of **1** was also successfully applied for sequential imaging of $Cu^{2+}$ and L-His in living cells. As shown in the upper row of Fig. 4, after the healthy HepG2 cells were incubated with 10 μM **1** in serum-free culture medium at 37 °C for 1 h and washed three times with phosphate buffered saline (PBS, pH 7.4) to remove the free **1**, bright green fluorescence cell imaging could be observed. This suggests that our water soluble probe **1** has much better cell permeability than FITC and is suitable for live cell imaging (Fig. S11, ESI†). After that, 20 μM $Cu^{2+}$ was added to the medium and incubated

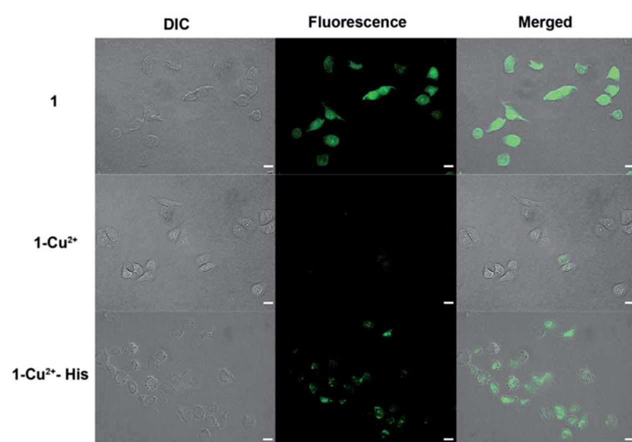


Fig. 4 Differential interference contrast (DIC) images (left), fluorescence images (middle, EGFP channel), and merged images (right) of HepG2 cells incubated with 10 μM of probe **1** in serum-free medium for 1 h at 37 °C, washed with PBS three times prior to imaging (upper row), incubated with 20 μM $Cu^{2+}$ in serum-free medium for 20 min at 37 °C prior to imaging (middle row), then incubated with 200 μM L-His in serum-free medium for 20 min at 37 °C prior to imaging (lower row), respectively. Scale bar: 20 μm.

 This journal is © The Royal Society of Chemistry 2014

Published on 17 April 2014. Downloaded by University of Science and Technology of China on 12/01/2015 02:05:50.

with the cells for 20 min at 37 °C prior to imaging. Obviously we found the fluorescence emission from the cells was dimmed out (middle row of Fig. 4). The process of this fluorescence "dimming out" was clearly observed by incubating the cells with increasing $Cu^{2+}$ concentrations (Fig. S12, ESI†). The highest concentration of $Cu^{2+}$ in our cell study (*i.e.*, 20 μM) should be far below that inducing cytotoxicity.[23] Interestingly, after subsequent addition of 200 μM of L-His to the culture medium and the cells were incubated for another 20 min, we found the fluorescence emission from the cells was turned "on" again (low row of Fig. 4). Interestingly, from Fig. 4, we found that the subcellular distribution of **1** in the **1**-treated cells alone was different from that in the **1**–$Cu^{2+}$–L-His-treated cells, suggesting that **1** is not ratiometric to each individual cell. Additional experiments indicated that the recovery of the fluorescence of the **1**–$Cu^{2+}$ complex was not induced by small molecules inside cells such as glutathione (GSH) (Fig. S13, ESI†). The process of the fluorescence "turn-on" was also monitored by incubating the cells with increasing L-His concentrations (Fig. S16, ESI†).

## Conclusions

In conclusion, we have successfully developed a new fluorescent switch for sequential and selective detection of $Cu^{2+}$ and L-His *in vitro* and in living cells. The new water-soluble and cell-permeable probe **1** has a SAACQ motif for $Cu^{2+}$ chelation and its fluorescence from the fluorophore FITC can be quenched *via* a PET mechanism after $Cu^{2+}$ chelation. This property was successfully applied for highly selective $Cu^{2+}$ detection within the range of 0–10 μM and a LOD of 0.24 μM. Interestingly, the formed **1**–$Cu^{2+}$ complex could be applied for selective detection of L-His within 1–60 μM among the twenty natural AAs with a LOD of 1.6 μM. With the excellent properties of **1** for the detection of $Cu^{2+}$ and L-His with high selectivity, we also successfully applied it for sequential imaging of $Cu^{2+}$ and L-His in living cells. We hope that our new dual functional probe **1** could be applied for not only environmental monitoring but also for biomolecule detection in the near future.[24]

## Acknowledgements

This work was supported by the National Natural Science Foundation of China (Grants 21175122, 91127036, and 21375121) and the Fundamental Research Funds for Central Universities (WK2060190018).

## Notes and references

1 B. E. Kim, T. Nevitt and D. J. Thiele, *Nat. Chem. Biol.*, 2008, **4**, 176–185.
2 R. Uauy, M. Olivares and M. Gonzalez, *Am. J. Clin. Nutr.*, 1998, **67**, 952s–959s.
3 B. Schleper and H. J. Stuerenburg, *J. Neurol.*, 2001, **248**, 705–706.
4 (*a*) B. P. Zietz, H. H. Dieter, M. Lakomek, H. Schneider, B. Kessler-Gaedtke and H. Dunkelberg, *Sci. Total Environ.*, 2003, **302**, 127–144; (*b*) G. Georgopoulos, A. Roy, M. J. Yonone-Lioy, R. E. Opiekun and P. J. Lioy, *J. Toxicol. Environ. Health, Part B*, 2001, **4**, 341–394.
5 (*a*) Y. Zheng, J. Orbulescu, X. Ji, F. M. Andreopoulos, S. M. Pham and R. M. Leblanc, *J. Am. Chem. Soc.*, 2003, **125**, 2680–2686; (*b*) M. Boiocchi, L. Fabbrizzi, M. Licchelli, D. Sacchi, M. Vazquez and C. Zampa, *Chem. Commun.*, 2003, 1812–1813; (*c*) H. S. Jung, P. S. Kwon, J. W. Lee, J. I. Kim, C. S. Hong, J. W. Kim, S. Yan, J. Y. Lee, J. H. Lee, T. Joo and J. S. Kim, *J. Am. Chem. Soc.*, 2009, **131**, 2008–2012; (*d*) S. Sirilaksanapong, M. Sukwattanasinitt and P. Rashatasakhon, *Chem. Commun.*, 2012, **48**, 293–295; (*e*) J. L. Yao, K. Zhang, H. J. Zhu, F. Ma, M. T. Sun, H. Yu, J. Sun and S. H. Wang, *Anal. Chem.*, 2013, **85**, 6461–6468; (*f*) Y. Zhao, X. B. Zhang, Z. X. Han, L. Qiao, C. Y. Li, L. X. Jian, G. L. Shen and R. Q. Yu, *Anal. Chem.*, 2009, **81**, 7022–7030; (*g*) A. C. Liu, D. C. Chen, C. C. Lin, H. H. Chou and C. H. Chen, *Anal. Chem.*, 1999, **71**, 1549–1552; (*h*) N. Kumar, V. Bhalla and M. Kumar, *Analyst*, 2014, **139**, 543–558.
6 J. F. Wu and E. A. Boyle, *Anal. Chem.*, 1997, **69**, 2464–2470.
7 (*a*) S. Caroli, A. Alimonti, F. Petrucci and Z. Horvath, *Anal. Chim. Acta*, 1991, **248**, 241–249; (*b*) J. F. Wu and E. A. Boyle, *Anal. Chem.*, 1997, **69**, 2464–2470; (*c*) S. Tokalioglu, S. Kartal and L. Elci, *Anal. Chim. Acta*, 2000, **413**, 33–40; (*d*) B. Y. Deng, Y. Z. Wang, P. C. Zhu, X. S. Xu and X. Ning, *Anal. Chim. Acta*, 2010, **683**, 58–62.
8 S. Lee, I. Choi, S. Hong, Y. I. Yang, J. Lee, T. Kang and J. Yi, *Chem. Commun.*, 2009, 6171–6173.
9 S. Sarkar, M. Pradhan, A. K. Sinha, M. Basu and T. Pal, *Chem. - Eur. J.*, 2012, **18**, 6335–6342.
10 (*a*) L. Feng, H. Li, Y. Lv and Y. Guan, *Analyst*, 2012, **137**, 5829–5833; (*b*) A. Ganguly, B. K. Paul, S. Ghosh, S. Kar and N. Guchhait, *Analyst*, 2013, **138**, 6532–6541; (*c*) S. Sarkar, S. Roy, A. Sikdar, R. N. Saha and S. S. Panja, *Analyst*, 2013, **138**, 7119–7126; (*d*) R. Krämer, *Angew. Chem., Int. Ed.*, 1998, **37**, 772–773; (*e*) J. Du, M. Hu, J. Fan and X. Peng, *Chem. Soc. Rev.*, 2012, **41**, 4511–4535; (*f*) J. Jo, H. Y. Lee, W. J. Liu, A. Olasz, C. H. Chen and D. Lee, *J. Am. Chem. Soc.*, 2012, **134**, 16000–16007; (*g*) C. F. Monson, X. Cong, A. D. Robison, H. P. Pace, C. M. Liu, M. F. Poyton and P. S. Cremer, *J. Am. Chem. Soc.*, 2012, **134**, 7773–7779; (*h*) L. Zeng, E. W. Miller, A. Pralle, E. Y. Isacoff and C. J. Chang, *J. Am. Chem. Soc.*, 2006, **128**, 10–11; (*i*) M. T. Morgan, P. Bagchi and C. J. Fahrni, *J. Am. Chem. Soc.*, 2011, **133**, 15906–15909; (*j*) Y. Fu, C. Q. Ding, A. W. Zhu, Z. F. Deng, Y. Tian and M. Jin, *Anal. Chem.*, 2013, **85**, 11936–11943; (*k*) D. W. Domaille, L. Zeng and C. J. Chang, *J. Am. Chem. Soc.*, 2010, **132**, 1194–1195.
11 (*a*) J. Liu and Y. Lu, *J. Am. Chem. Soc.*, 2007, **129**, 9838–9839; (*b*) J. W. Liu, Z. H. Cao and Y. Lu, *Chem. Rev.*, 2009, **109**, 1948–1998; (*c*) Z. Y. Fang, J. Huang, P. C. Lie, Z. Xiao, C. Y. Ouyang, Q. Wu, Y. X. Wu, G. D. Liu and L. W. Zeng, *Chem. Commun.*, 2010, **46**, 9043–9045.
12 F. A. Settle, in *Handbook of Instrumental Techniques for Analytical Chemistry*, Prentice Hall, New Jersey, 1997.
13 (*a*) X. Lou, L. Zhang, J. Qin and Z. Li, *Langmuir*, 2010, **26**, 1566–1569; (*b*) R. J. Sundberg and R. B. Martin, *Chem. Rev.*,

Published on 17 April 2014. Downloaded by University of Science and Technology of China on 12/01/2015 02:05:50.

1974, **74**, 471–517; (*c*) P. Deschamps, P. P. Kulkarni, M. Gautam-Basak and B. Sarkar, *Coord. Chem. Rev.*, 2005, **249**, 895–909.

14 B. Sarkar, *Chem. Rev.*, 1999, **99**, 2535–2544.

15 M. Jaksch, C. Paret, R. Stucka, N. Horn, J. Muller-Hocker, R. Horvath, N. Trepesch, G. Stecker, P. Freisinger, C. Thirion, J. Muller, R. Lunkwitz, G. Rodel, E. A. Shoubridge and H. Lochmuller, *Hum. Mol. Genet.*, 2001, **10**, 3025–3035.

16 (*a*) X. H. Li, H. M. Ma, S. Y. Dong, X. J. Duan and S. C. Liang, *Talanta*, 2004, **62**, 367–371; (*b*) X. H. Li, H. M. Ma, L. H. Nie, M. Sun and S. X. Xiong, *Anal. Chim. Acta*, 2004, **515**, 255–260; (*c*) M. A. Hortala, L. Fabbrizzi, N. Marcotte, F. Stomeo and A. Taglietti, *J. Am. Chem. Soc.*, 2003, **125**, 20–21.

17 K. A. Stephenson, J. Zubieta, S. R. Banerjee, M. K. Levadala, L. Taggart, L. Ryan, N. McFarlane, D. R. Boreham, K. P. Maresca, J. W. Babich and J. F. Valliant, *Bioconjugate Chem.*, 2004, **15**, 128–136.

18 Y. Yang, Q. Zhao, W. Feng and F. Li, *Chem. Rev.*, 2013, **113**, 192–270.

19 R. Huang, X. Wang, D. Wang, F. Liu, B. Mei, A. Tang, J. Jiang and G. Liang, *Anal. Chem.*, 2013, **85**, 6203–6207.

20 X. M. He, N. Y. Zhu and V. W. W. Yam, *Organometallics*, 2009, **28**, 3621–3624.

21 T. D. Rae, P. J. Schmidt, R. A. Pufahl, V. C. Culotta and T. V. O'Halloran, *Science*, 1999, **284**, 805–808.

22 L. An, L. Liu and S. Wang, *Biomacromolecules*, 2009, **10**, 454–457.

23 (*a*) Y. You, Y. Han, Y. M. Lee, S. Y. Park, W. Nam and S. J. Lippard, *J. Am. Chem. Soc.*, 2011, **133**, 11488–11491; (*b*) M. Yu, M. Shi, Z. Chen, F. Li, X. Li, Y. Gao, J. Xu, H. Yang, Z. Zhou, T. Yi and C. Huang, *Chem. - Eur. J.*, 2008, **14**, 6892–6900.

24 Y. Yuan, S. L. Jiang, Q. Q. Miao, J. Zhang, M. J. Wang, L. N. An, Q. J. W. Cao, Y. F. Guan, Q. Zhang and G. L. Liang, *Talanta*, 2014, **125**, 204–209.

 This journal is © The Royal Society of Chemistry 2014